

Sol-gel auto-combustion synthesis and LPG sensing performance of $Mg_{(x)}Fe_{(1-x)2}O_4$ nanoparticles

A. Akshaykranth*, R. Karthik* and K. Venkateswara Rao**,
C.H. Shilpa Chakra**

ABSTRACT

This work provides a comprehensive study of the mesoporous $Mg_{(x)}Fe_{(1-x)2}O_4$ nanoparticles synthesized via sol-gel auto-combustion method. The main objective of the current research is to influence by increasing the concentration of ferrite with magnesium in nanostructure $Mg_{(x)}Fe_{(1-x)2}O_4$ ($X=0.1, 0.2, 0.3, 0.4, 0.5, 0.6, 0.7, 0.8$ and 0.9) and carry out the investigation with exposed to Liquid petroleum gas (LPG). The prepared $Mg_{(x)}Fe_{(1-x)2}O_4$ samples were characterized using XRD, Scanning electron microscope, UV-Visible spectroscopy, Particle Size Analyzer. The nanostructured $Mg_{(x)}Fe_{(1-x)2}O_4$ ($x=0.1, 0.5$ and 0.9) films deposited by spin coating technique, has been studied for sensing performance towards LPG at 500 ppm at different operating temperatures.

Keywords: Ferrites; Porosity; PSA; Gas Sensors; LPG.

1. INTRODUCTION

Spinel ferrites are having important electrical and magnetic properties. Nano ferrites materials offer more sensitivity, selectivity and long-term stable sensor material. $MgFe_2O_4$ gas sensors have important parameters such as phase formation, crystalline size, size of the particle and grain, surface area etc. Magnesium ferrite, $MgFe_2O_4$ is regarded as an essential candidate of the spinel family. It has a cubic structure of the normal spinel type and is a soft magnetic n-type semiconducting material, which finds a wide number of applications in heterogeneous catalysis [1], gas sensors [2], transformers, Ferro fluids and magnet core of coils [3]. Among various materials used for sensing application, ferrite is used as a good class of sensing materials.

Liang-Dong Feng *et al* reported that Sr-doped SnO_2 thick film sensors were prepared using screen-printing technique and high sensitivity of 12.7 in the temperature range 210-300°C for detection of 10ppm concentration of LPG [4]. Sumanta Kumar Tripathy *et al* reported that Semiconducting tin oxide (SnO_2) thin film was synthesized on glass substrate by Sol-gel dip coating method. The thickness of the film was 645.98nm and grain size was 48.5nm. The sensitivity of the film was more for 50ppm of CO Gas concentration at 220°C temperature and response time is 20s [5]. Chaugule V V *et al* used Bacillus subtilis and nano crystalline $MgFe_2O_4$ which was synthesized by self-combustion route. Bacillus subtilis $MgFe_2O_4$ thick bio-film has noticed highest response of 20s for 300ppm of CO_2 gas concentration at 370°C temperature [6]. Sachin Bangale *et al* reported that Escherichia coli- $MgFe_2O_4$ synthesis route employed in this study may also be used for the synthesis of other bacterial cells and metal oxides respectively. A response of 30s at 30ppm concentration of ammonia at 37°C was observed. The applied sensor showed rapid response and fast recovery to ammonia gas. The sensor has good selectivity to ammonia compared to ethanol, acetone, CO_2 and LPG [7]. Sachin Bangale *et al* reported that Pseudomonas aeruginosa $MgFe_2O_4$ noticed highest

* Dept. of Electronics & Communication Engineering, MLR Institute of Technology, Hyderabad, India, *Emails:* akshaykranth417@gmail.com karthik.r@mlrinstitutions.ac.in

** Centre for Nanoscience & Technology IST – JNTU Hyderabad, Hyderabad, India.

response at 30ppm concentration of H_2S at $370^\circ C$ temperature. Also, response time, recovery time was 17s, 55s respectively [8]. Sonali L. Darshane *et al* reported that Single-phase nanocrystallite (H^{16} nm) spinel zinc ferrite was obtained from the environment-friendly simple molten salt route at a relatively low processing temperature and for a short duration. The sensor based on this material exhibits a marked selective response time of 30s toward 200 ppm of H_2S at $250^\circ C$ [9]. P Samarasekara *et al* reported that the CO_2 gas sensitivity of the film synthesized at a substrate temperature of $130^\circ C$ was measured to be 2.17 at $100^\circ C$. The gas sensitivity at N_2 has been investigated to study the cross-sensitivity. The response and recovery time of this film were 5s and 10 min, respectively for CO_2 [10].

P P Sahay *et al* reported that Al-doped zinc oxide thin films prepared by chemical spray pyrolysis technique have been studied for LPG sensors. The 0.5 % of Al-doped ZnO film shows the maximum response (<“89%) at $325^\circ C$ to 1vol% LPG in air, whereas in the case of undoped ZnO, the response is found to be about 40% at the same operating temperature and concentration of LPG in air [11]. G S Trivikrama Rao *et al* reported that thick film ammonia gas sensor elements with and without dopants were prepared and characterized. Among all of the devices tested, the Pd–ZnO exhibited good sensitivity and response time to NH_3 at room temperature. The gas sensitivities to 30 ppm of NH_3 of ZnO (Pd), ZnO, ZnO (Fe) and ZnO (Ru) were 60, 35, 25 and 10%, respectively [12].

Lalchand A. Patil *et al* reported that Pure ZnO thick films were observed to be less sensitive to NH_3 gas even at higher temperature. MnO_2 modified ZnO sensors showed crucial response to NH_3 gas at room temperature. The sensor was highly selective to NH_3 gas (50 ppm) against other toxic gases of higher concentrations (1000 ppm). The sensor showed very rapid response time 10s and recovery time 50s to NH_3 gas [13]. D R Patil *et al* reported that Pure ZnO thick films were observed to be sensitive to NH_3 gas but at higher temperature. Cr_2O_3 -activated ZnO sensors showed crucial response to NH_3 gas at room temperature. The sensor was highly selective to NH_3 gas (300 ppm) against other toxic gases of higher concentrations [14].

2. MATERIAL PREPARATION

2.1. Synthesis of $Mg_x Fe_{(1-x)2} O_4$ nanoparticles

The $Mg_x Fe_{(1-x)2} O_4$ powders were prepared by using sol gel auto combustion synthesis. The materials used as precursors were Magnesium nitrate hexahydrate $Mg(NO_3)_2 \cdot 6H_2O$, Iron nitrate hexahydrate $Fe(NO_3)_3 \cdot 9H_2O$ and glycine (Sigma Aldrich). All of them were of high purity (99.9 %). Glycine possesses a high heat of combustion. It is an organic fuel providing a platform for redox reactions during the course of combustion. Magnesium nitrate and Iron nitrate were dissolved in separate 500ml Beaker with each 25ml of Distilled Water and keep stirring for 20 min, after that add both chemicals slowly with Glycine and keep stirring for 30min. The accurate weight of each chemical taken for total Magnesium ferrite series $Mg_x Fe_{(1-x)2} O_4$ ($X= 0.1$ to 0.9). Then keep the beaker on hot plate and maintain $80^\circ C$ to $100^\circ C$ to form thick gel. Later, increase and maintain the temperature range of $180^\circ C$ to $200^\circ C$. Slowly fumes & flames will be seen due to the above procedure. The nanocrystalline $Mg_x Fe_{(1-x)2} O_4$ powders were formed within a few minutes and it was sintered at about $650^\circ C$ for 4 hours. The color of each Magnesium Ferrite was different in the series of $Mg_x Fe_{(1-x)2} O_4$ ($X= 0.1$ to 0.9) [15]. The sintered Magnesium Ferrite samples were used for thin film coating using Spin Coater.

2.2. Fabrication of thin film

$Mg_x Fe_{(1-x)2} O_4$ ($x=0.1$ to 0.9) thin films were deposited onto well cleaned silicon substrate using a conventional spin coater system. Before coating, a gel kind of solution was prepared by adding of Hydroxyethyl cellulose (HEC) 100mg to 5ml of methanol and 5ml of distilled water and stirred for 1hour at room temperature. Later, this was mixed with 300mg of magnesium ferrite. This resulted in a viscous gel which was used for

thin film coating at 3000 rpm in spin coater. Next, the thin films were dried and annealed in different temperatures. The obtained film was then used for the sensing after adding silver contacts by dropping technique.

3. RESULTS AND DISCUSSION

3.1. Characterization of $Mg_{(x)}Fe_{(1-x)2}O_4$ nanoparticles

Figure 1 shows the XRD pattern of $Mg_{(x)}Fe_{(1-x)2}O_4$ series prepared by sol-gel auto combustion with fuel to oxidizer ratio of $\phi=1$. It is observed that in $Mg_{(x)}Fe_{(1-x)2}O_4$ series $x=0.5$ sample matches with JCPDS 71-1232. The lattice parameters were obtained at $a=b=c=0.83\text{nm}$ and cubic structure. Remaining samples such as $x=0.1, 0.2, 0.3, 0.4, 0.6, 0.7, 0.8$ and 0.9 did not match with JCPDS number due to its oxidizer percentages in the respective samples. The $Mg_{(0.5)}Fe_{(0.5)2}O_4$ ($x=0.5$) sample has equal ratio of Magnesium and iron Percentages. X-ray diffracted peaks are corresponding to the planes (2 2 0), (3 1 1), (4 0 0), (4 2 2), (5 1 1) and (4 4 0) observed at $30^\circ, 35^\circ, 43^\circ, 54^\circ, 57^\circ$ and 62° respectively as shown in Figure1. The average crystallite size was measured by Debye-Scherer's equation as mentioned below,

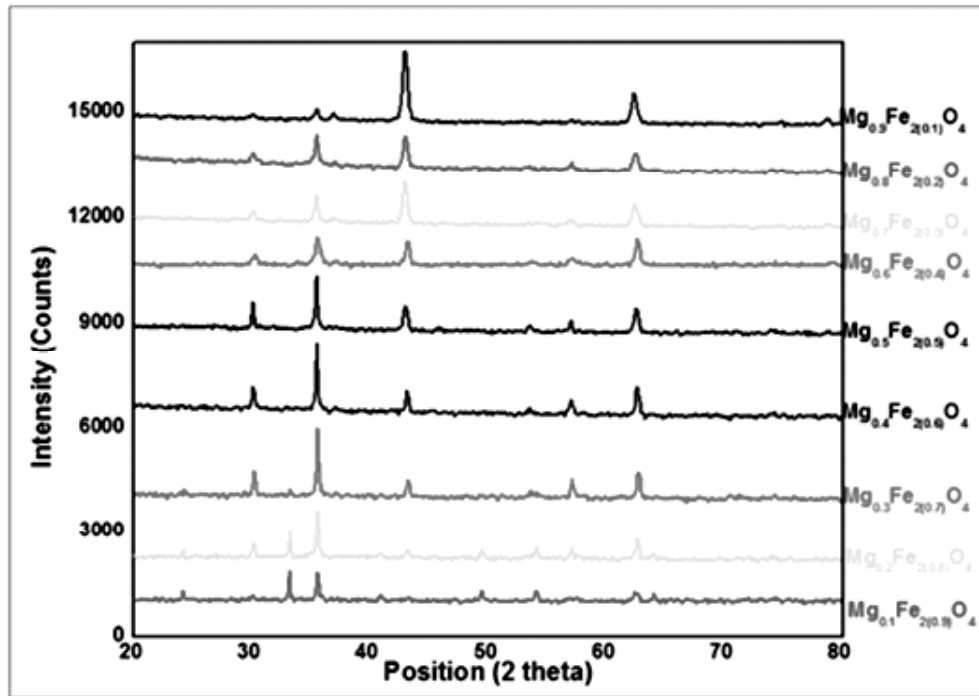
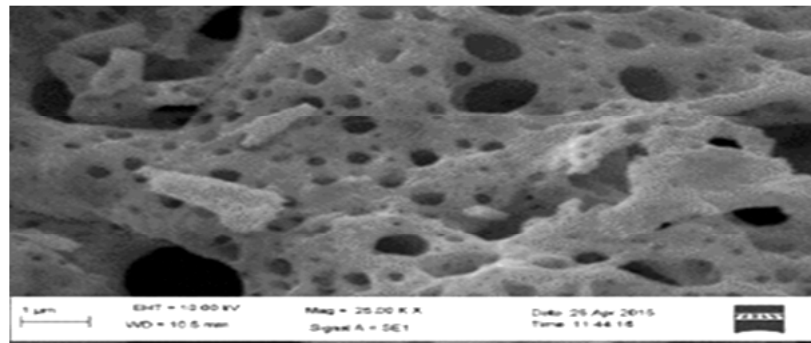


Figure 1: XRD pattern of $Mg_{(x)}Fe_{(1-x)2}O_4$ series prepared by sol-gel auto combustion with fuel to oxidizer ratio $\Psi=1$.

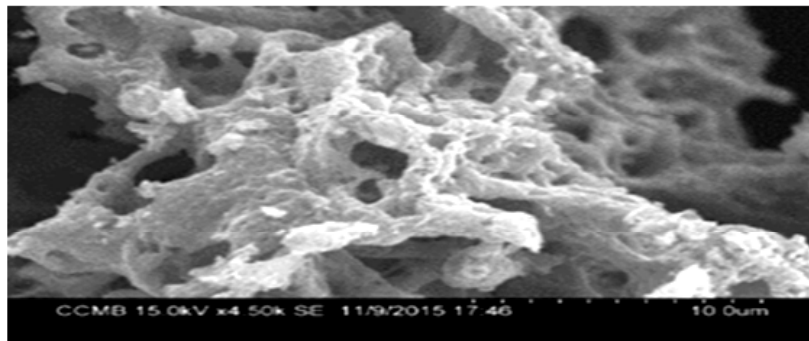
$$D = \frac{K\lambda}{\beta \cos\theta} \quad (1)$$

Where D is the average crystallite size of the particles, K is Debye Scherer's constant ($= 0.94$), λ is the wavelength of the $\text{Cu K}\alpha$ - radiation ($=0.154 \text{ nm}$), β is the full width half maximum (FWHM) of the peak and θ is the Bragg's angle [16-20]. The crystalline size estimated using Scherer formula is in the range of 12-24 nm.

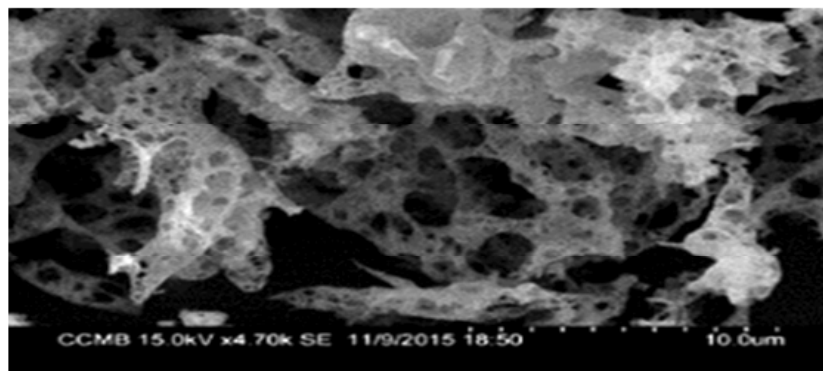
Figure 2 shows the SEM Images of various Magnesium Ferrite samples at $x=0.1, 0.5$ and 0.9 . It is observed that the $Mg_{(x)}Fe_{(1-x)2}O_4$ ($x=0.1, 0.5, 0.9$) nanoparticles showed remarkable change in the structure with respect to porosity, grain size of sample. It has frothy and small holes within structure, which may be due to escaping large number of gases during the combustion. The porosity in all cases is found to be entirely intergranular and shows high porous structure in nature. It is observed that the porosity of the



(a)



(b)



(c)

Figure 2: SEM Images of Magnesium Ferrite (a) $\text{Mg}_{0.5}\text{Fe}_{(0.5)2}\text{O}_4$, (b) $\text{Mg}_{0.1}\text{Fe}_{(0.9)2}\text{O}_4$, (c) $\text{Mg}_{0.9}\text{Fe}_{(0.1)2}\text{O}_4$.

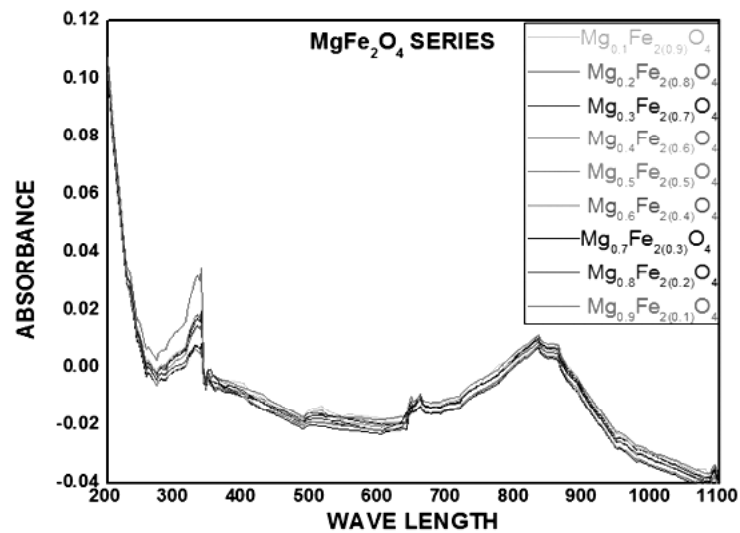
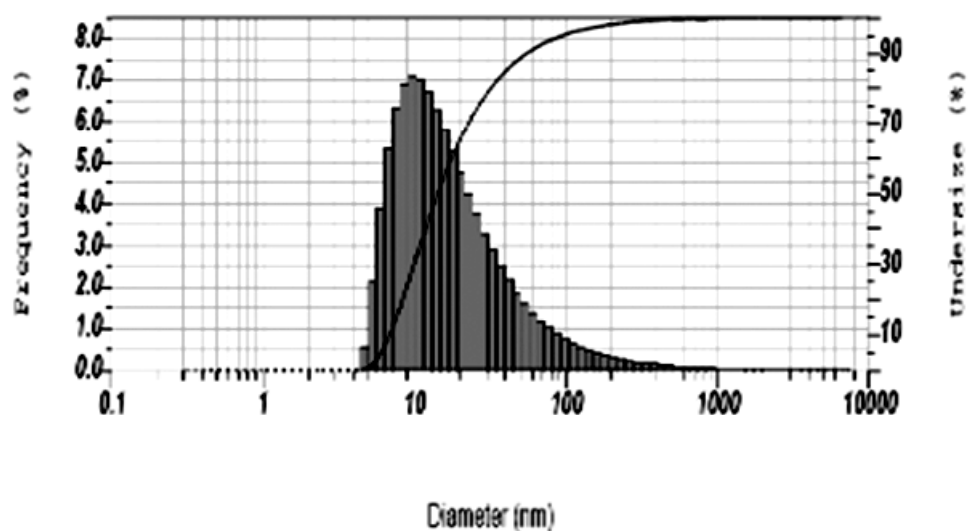


Figure 3: Reflectance spectra of $\text{Mg}_{(x)}\text{Fe}_{(1-x)2}\text{O}_4$ ($x=0.1$ to 0.9) nanoparticles

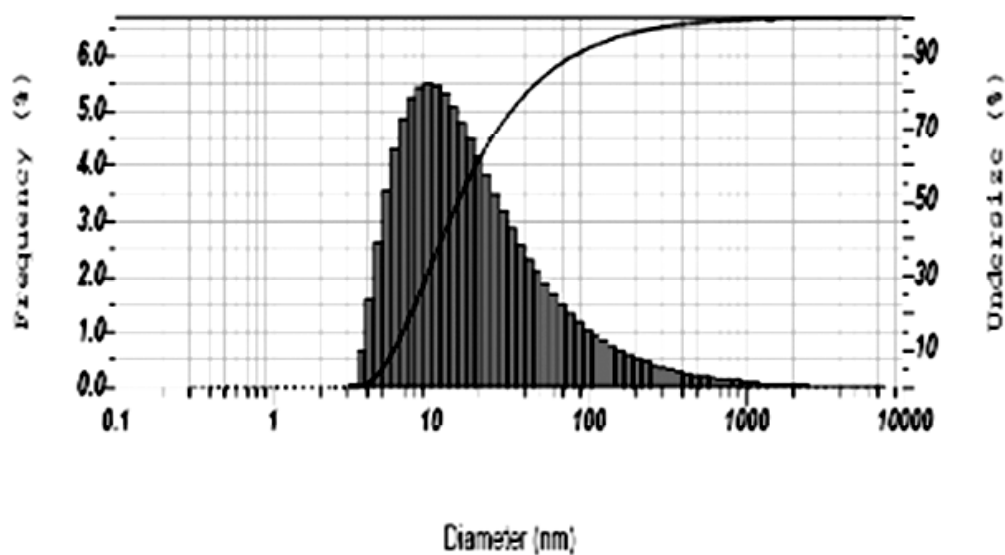
samples will increase when the magnesium percentage is increased (0.1 to 0.9) while decreasing the percentage of ferrite (0.9 to 0.1). This can be observed from Figure 2. In the $\text{Mg}_{(0.5)}\text{Fe}_{(0.5)2}\text{O}_4$ ($x=0.5$) sample, the porosity observed was around 200 nm.

Figure 3 shows the Reflectance spectra of $\text{Mg}_{(x)}\text{Fe}_{(1-x)2}\text{O}_4$ ($x=0.1$ to 0.9) nanoparticles. The optical properties of $\text{Mg}_{(x)}\text{Fe}_{(1-x)2}\text{O}_4$ ($x=0.1$ to 0.9) are investigated by UV-visible absorption spectroscopy. The reflectance spectra of pure and magnesium ferrite nanoparticles were analyzed in the spectral range of 300–900 nm. It is clear that all the samples show optical properties in the visible region. In pure $\text{Mg}_{(x)}\text{Fe}_{(1-x)2}\text{O}_4$ ($x=0.5$) sample, the reflectance percentage decreases with equal ratio of Mg-Fe percentage. But in the case of remaining samples, $\text{Mg}_{(x)}\text{Fe}_{(1-x)2}\text{O}_4$ ($x=0.1, 0.2, 0.3, 0.4, 0.6, 0.7, 0.8$ and 0.9) reflectance percentage was almost equal. All the samples in the series showed two peaks around 338 nm and 833 nm wavelength.

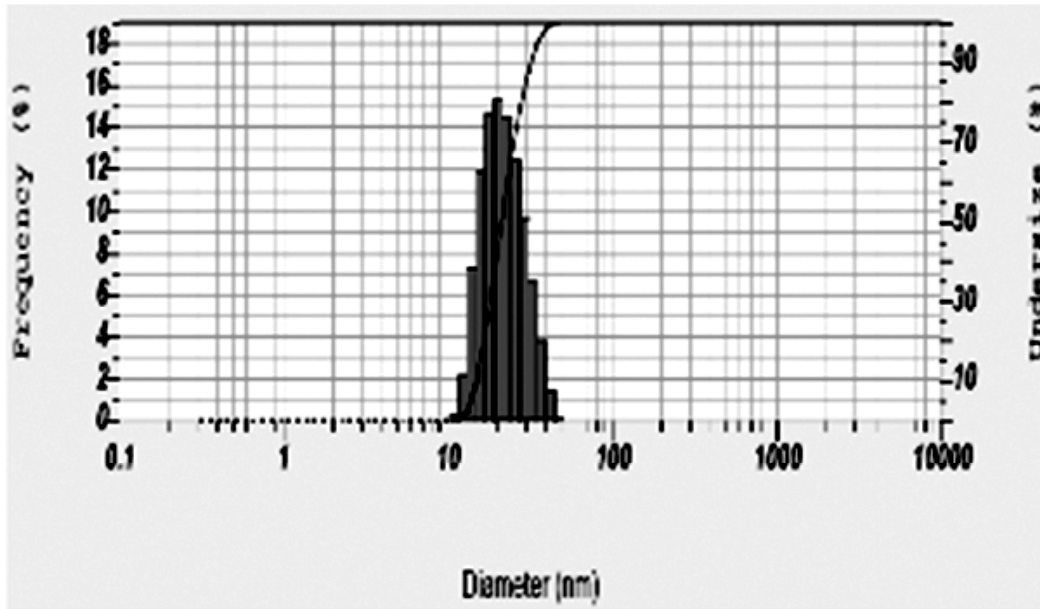
Figure 4 shows the particle size analyzer histograms of Magnesium Ferrite $\text{Mg}_{(x)}\text{Fe}_{(1-x)2}\text{O}_4$ ($x=0.1, 0.5$ and 0.9). It was observed from the particle size analyzer that the average particle size was obtained for $\text{Mg}_{(x)}\text{Fe}_{(1-x)2}\text{O}_4$ ($x=0.1, 0.5$ and 0.9) as 34.7 nm, 38.2 nm, and 22.5 nm, respectively. From this result, $\text{Mg}_{0.9}\text{Fe}_{2(0.1)}\text{O}_4$ shows the least average particle size. Hence, these results were supported to XRD average crystallite size.



(a)



(b)



(c)

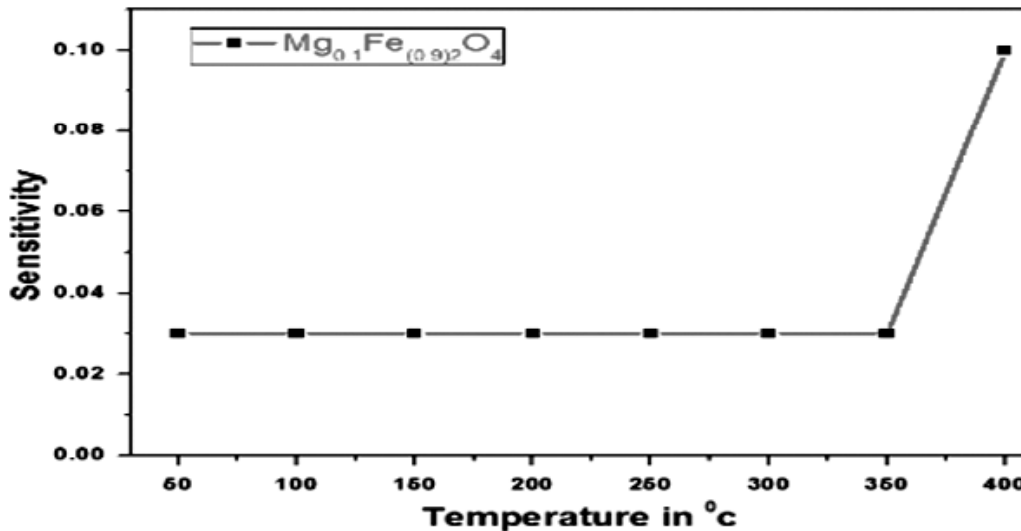
Figure 4: Particle size Analyzer Histograms of Magnesium Ferrite

(a) $\text{Mg}_{0.1}\text{Fe}_{(0.9)2}\text{O}_4$, (b) $\text{Mg}_{0.5}\text{Fe}_{(0.5)2}\text{O}_4$ (c) $\text{Mg}_{0.9}\text{Fe}_{(0.1)2}\text{O}_4$

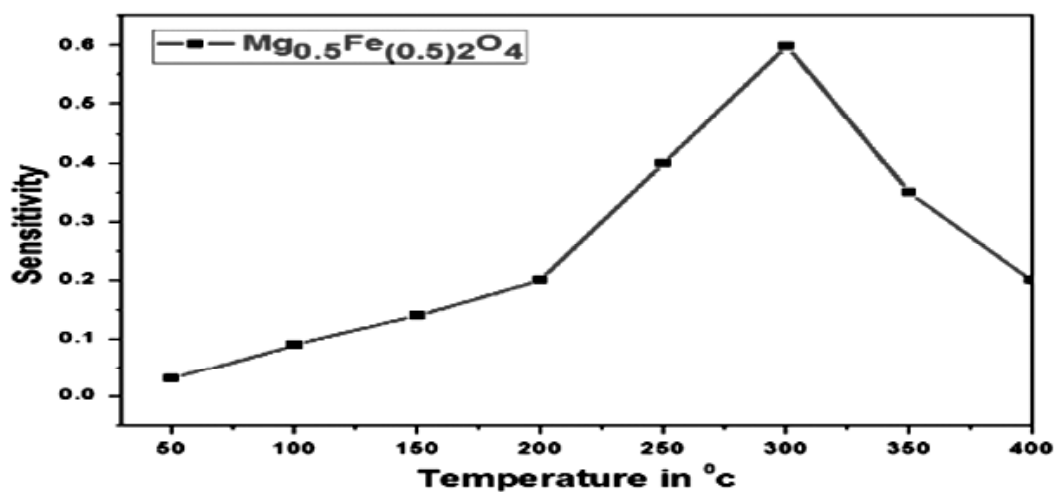
3.2. Performance of sensing for 500 ppm LPG

As discussed above, the sensing film was maintained at a temperature of 50 °C to 400 °C in a closed chamber and was degassed using rotary pump. In order to create atmospheric pressure inside the chamber synthetic air is admitted in to the chamber. The film resistance at the point of time is taken as base resistance (R_{air}). Consequently, when 500 ppm concentration of LPG is introduced in to the chamber, the chemisorption process will take place on the surface of $\text{Mg}_{(x)}\text{Fe}_{(1-x)2}\text{O}_4$ ($x=0.1, 0.5$ and 0.9) samples. This will increase the resistance of the films. The change in the film resistance at saturation point is R_{gas} . The factors effect Resistance are operating temperature, sensing element, concentration of LPG, ohmic contacts etc. The sensitivity was calculated using Equation 2,

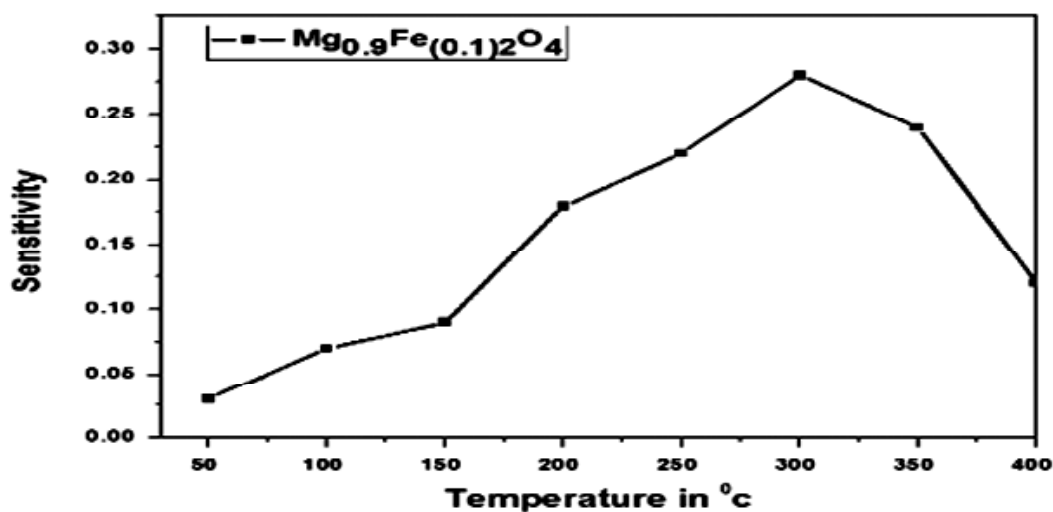
$$\text{Sensitivity} = [(R_{\text{air}} - R_{\text{gas}}) / R_{\text{air}}] \quad (2)$$



(a)



(b)



(c)

Figure 5: Sensitivity of Magnesium Ferrite (a) $Mg_{0.1}Fe_{(0.9)2}O_4$, (b) $Mg_{0.5}Fe_{(0.5)2}O_4$, (c) $Mg_{0.9}Fe_{(0.1)2}O_4$ films for 500 ppm LPG at different temperature ranges.

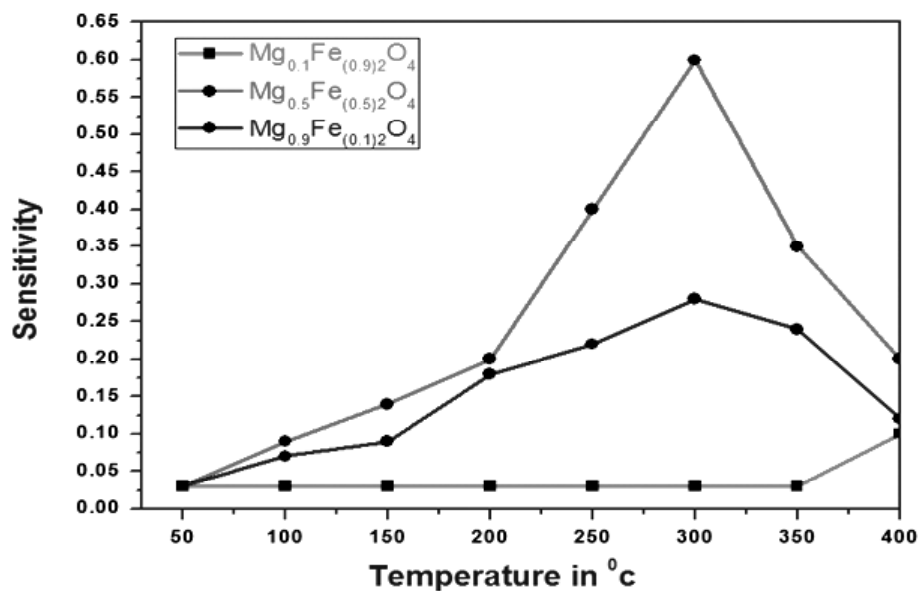


Figure 6: A comparative graph of $Mg_xFe_{(1-x)2}O_4$ ($x=0.1, 0.5$ and 0.9) samples for sensitivity at 500 ppm LPG.

Figure 6 shows the comparative graph of Magnesium ferrite samples for sensitivity at 500ppm LPG. It was observed that the sensitivity of $\text{Mg}_{(0.5)}\text{Fe}_{(0.5)2}\text{O}_4$ was high compared to the remaining two samples. The sensing response was calculated by measuring change in resistance. Using the Pico ammeter at fixed bias voltage of 2V, it was observed that sensitivity is 0.6 for $\text{Mg}_{(0.5)}\text{Fe}_{(0.5)2}\text{O}_4$ sample. It was high due to equal percentage of Mg-Fe ratio compared to remaining two samples $\text{Mg}_{(x)}\text{Fe}_{(1-x)2}\text{O}_4$ ($x=0.1$ and 0.9).

4. CONCLUSION

In this work, nanoparticles of $\text{Mg}_{(x)}\text{Fe}_{(1-x)2}\text{O}_4$ ($x=0.1$ to 0.9) are synthesized using sol-gel (auto combustion) route with a view to understand the changes of properties in the Nano regime. Nanoparticles of $\text{Mg}_{(x)}\text{Fe}_{(1-x)2}\text{O}_4$ were observed to be in the form of mixed spinels. Structural, morphological and optical properties are studied successfully by changing the concentration of the Mg-Fe percentage. This performance study on the different concentration of $\text{Mg}_{(x)}\text{Fe}_{(1-x)2}\text{O}_4$ ($x=0.1, 0.5$ and 0.9) will be helpful for the optimization of various important parameters such as operating temperatures and sensitivity to LPG sensor.

ACKNOWLEDGMENT

The authors express their deep sense of gratitude to Dr. K Venkateshwara Rao and Dr. CH Shilpa Chakra, Centre for Nano Science and Technology, IST, JNTU-Hyderabad for giving this opportunity to carry out the Synthesis, Fabrication and Characterization works at CNST department.

REFERENCES

- [1] B.L.Yang, D.S. Cheng and S.B. Lee, "Effect of steam on the oxidative dehydrogenation of butene over magnesium ferrites with and without chromium substitution", *Applied Catalysis*, 70: 161-173, 1991.
- [2] Y.L.Liu, Z.M. Liu, Y. Yang, H.F. Yang, G.L. Shen and R.Q. Yu, "Simple synthesis of MgFe_2O_4 nanoparticles as gas sensing materials", *Sensors and Actuators B: Chemical*, 107: 600-604, 2005.
- [3] C.Liu, B. Zou, A.J. Rondinone and Z.J. Zhang, "Chemical Control of Superparamagnetic Properties of Magnesium and Cobalt Spinel Ferrite Nanoparticles through Atomic Level Magnetic Couplings", *J. Am. Chem. Soc.*, 26: 6263-6267, 2000.
- [4] Liang-Dong Feng, Xing-Jiu Huang, and Yang-Kyu Cho. "Dynamic determination of domestic liquefied petroleum gas down to several ppm levels using a Sr-doped SnO_2 thick film gas sensor" *Microchim Acta* 156, 245–251, 2007.
- [5] Sumanta Kumar Tripathy, and Bhabani Prasad Hota "Carbon Monoxide Sensitivity of Tin Oxide Thin Film Synthesized by Sol Gel Method" *The African Review of Physics* 7:0047, 2012.
- [6] V.V.Chaugule And Bangale S.V "Microbial Gas Sensing Property of Bacillus Subtilis with Mixed Metal Catalyst MgFe_2O_4 " *International Journal of Microbiology Research* ISSN: 0975-5276 & E-ISSN: 0975-9174, Vol. 3, Issue 3, 2011.
- [7] Sachin Bangale, Vinay Chaugule, Reshma Prakshale and Sambaji Bamane "Microbial gas-sensing property of Escherichia coli with mixed metal catalyst MgFe_2O_4 " *Research Communications Current Science*, Vol. 105, No. 7, 10 October 2013.
- [8] Sachin Bangale, Vinay Chaugule, Reshma prakshale, and Sambhaji Bamane "Microbial Gas sensing property of Pseudomonas aeruginosa with mixed metal catalyst MgFe_2O_4 " *RJPBCS Volume 4 Issue 1 Page No. 350, January-March 2013*.
- [9] L.Sonali, Darshane, Rupali G. Deshmukh, Shankar S. Suryavanshi, Imtiaz S. Mulla "Gas-Sensing Properties of Zinc Ferrite Nanoparticles Synthesized by the Molten-Salt Route" *J. Am. Ceram. Soc.*, 91 [8] 2724–2726, 2008.
- [10] P.Samarasekara, N U S Yapa, N T R N Kumara, M V K Perera, "Co₂ gas sensitivity of sputtered zinc oxide thin films", *Bull. Mater. Sci.*, Vol. 30, No. 2, pp. 113-116, April 2007.
- [11] P.P. Sahay, R.K. Nath "Al-doped zinc oxide thin films for liquid petroleum gas (LPG) sensors" *Sensors and Actuators B* 133 (2008) 222–227.
- [12] G.S. Trivikrama Rao 1, D. Tarakarama Rao "Gas sensitivity of ZnO based thick film sensor to NH₃ at room temperature" *Sensors and Actuators B* 55, 166–169.
- [13] Lalchand A. Patil, Lalita S. Sonawane, Dhanashri G. Patil "Room Temperature Ammonia Gas Sensing Using MnO₂-Modified ZnO Thick Film Resistors" *Journal of Modern Physics*, Vol 2, 1215-1221, 2011.
- [14] D.R. Patil, L.A. Patil, P.P. Patil "Cr₂O₃-activated ZnO thick film resistors for ammonia gas sensing operable at room temperature" *Sensors and Actuators B* 126 368–374, 2007.

- [15] Mohsen Ahmadipour, K. Venkateswara Rao “Preparation of Nano Particle $Mg_{0.2}Fe_{0.8}O$ by Solution Combustion Method and Their Characterization” International Journal of Engineering and Advanced Technology (IJEAT) ISSN: 2249 – 8958, Volume-1, Issue-6, November 2012.
- [16] N. M. Derazl, and Omar H. Abd-Elkader, “Effects of Magnesia Content on Spinel Magnesium Ferrite Formation”, Int. J. Electrochem. Sci., 8 8632 – 8644, 2013.
- [17] N. M. Derazl and Omar H. Abd-Elkader, “Investigation of Magnesium Ferrite Spinel Solid Solution with Iron-Rich Composition”, Int. J. Electrochem. Sci., 8, 9071 – 9081, 2007.
- [18] Abdul Gaffoor and D. Ravinder, “Characterization of Magnesium Substituted Nickel Nano Ferrites Synthesized By Citrate-Gel Auto Combustion Method”, Int. Journal of Engineering Research and Applications, ISSN : 2248-9622, Vol. 4, Issue 4(Version 8), pp. 60-66, April 2014.
- [19] A. A. Thant, S. Srimala, P. Kaung, M. Itoh, O. Radzali and M. N. Ahmad Fauzi, “Low Temperature Synthesis of $MgFe_2O_4$ Soft Ferrite Nanocrystallites” Journal of the Australian Ceramic Society Volume 46[1], 11-14, 2010.
- [20] Joseph Govha ,T. Bala Narasaiah, Pramod Kumar , Ch. Shilpa Chakra, “Synthesis of Nano-Magnesium Ferrite Spinel and its Characterization” International Journal of Engineering Research & Technology (IJERT), ISSN: 2278-0181, Vol. 3 Issue 8, August – 2014.

